analytical chemistry

Technical Note

pubs.acs.org/ac

Electrogenerated Chemiluminescence Peptide-Based Biosensor for the Determination of Prostate-Specific Antigen Based on Target-Induced Cleavage of Peptide

Honglan Qi,* Min Li, Manman Dong, Sanpeng Ruan, Qiang Gao, and Chengxiao Zhang*

Key Laboratory of Applied Surface and Colloid Chemistry, Ministry of Education, School of Chemistry and Chemical Engineering, Shaanxi Normal University, Xi'an, Shaanxi 710062, PR China

Supporting Information

ABSTRACT: A novel electrogenerated chemiluminescence peptide-based biosensor (ECL-PB) for the determination of prostate-specific antigen (PSA) was developed on the basis of target-induced cleavage of a specific peptide within Nafion film incorporated with gold nanoparticles (AuNPs) and ECL emitting species. A specific peptide (CHSSKLQK) was used as a molecular recognition element; tris(2,2′-ripyridine) dichlororuthenium(II) ($Ru(bpy)_3^{2+}$) was used as ECL emitting species, and ferrocene carboxylic acid (Fc) was employed as ECL quencher. The ECL-PB biosensor was fabricated by casting the mixture of Nafion and AuNPs onto the surface of glassy carbon electrode to form AuNPs/Nafion film, and then, $Ru(bpy)_3^{2+}$ was electrostatically adsorbed into the AuNPs/Nafion film; finally, the peptide-tagged with ferrocene carboxylic acid (Fc-peptide) was self-assembled onto the surface of the AuNPs. When PSA was present, it specifically cleaved the Fc-peptide, leading the quencher to leave the electrode and resulting in the increase of the ECL intensity obtained from the resulted electrode in 0.1 M phosphate buffer saline (pH 7.4) containing tri-*n*-propylamine. The results showed that the increased ECL intensity was directly linear to the logarithm of the concentration of PSA in the range from 5.0×10^{-12} to 5.0×10^{-9} g/mL. An extremely low detection limit of 8×10^{-13} g/mL was achieved because of the signal amplification through AuNPs and the ECL background suppression through Fc as ECL quencher. This work demonstrates that the combination of the direct transduction of peptide cleavage events with the highly sensitive ECL method is a promising strategy for the design of enzymatic cleavage-based ECL biosensors with high sensitivity and selectivity.

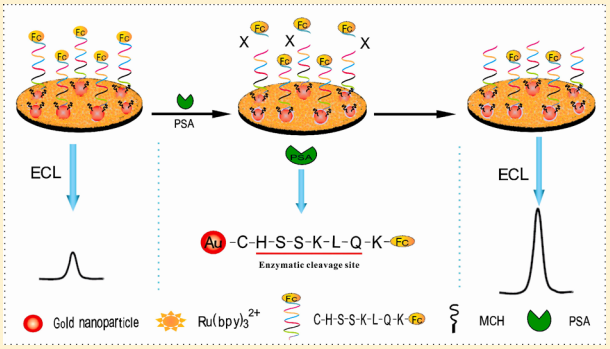

Development of simple, sensitive, and selective methods for the determination of specific proteins, especially, cancer biomarkers, has received more and more attention in clinical and biological fields.[1] Prostate-specific antigen (PSA), a sense protease secreted by both normal prostate glandular cells and prostate cancer cells,[2] has been identified as the most reliable tumor marker for the early diagnostics of prostate cancer and for monitoring the recurrence of the disease after treatment.[3,4] Although the cutoff value for PSA in the diagnostic of prostate cancer is 4.0 ng/mL (and more recently 2.5 ng/mL), ultrasensitive assays capable of detecting concentrations of serum PSA in the low pg/mL region have been sought to diagnose prostate cancer in the postsurgery recurrence.[5,6] Additionally, PSA is found in the sera of breast cancer patients, and it is beginning to be explored as a breast cancer screening target.[7] Because the concentration of PSA is much lower in women's serum as compared to that of men, the development of an ultrasensitive method for the determination of PSA is of great importance. A lot of the methods for the determination of PSA have been developed such as fluorescence,[8] surface plasmon resonance,[9] and electrochemical[10] and electrogenerated chemiluminescence (also called electrochemiluminescence and abbreviated ECL) immunoassay.[11−15] Despite the improvement of these methods, it is thought that PSA in blood measured by current routine immunoassays is inactive and the antibody drawbacks associated with its production in vivo, stability, and manipulation have prompted researchers to seek alternatives of antibody.[16]

Recently, short binding peptides, which are selected using the phage display technique, have been used as a promising alternative to conventional antibody in bioassays due to their advantages, such as being reliable, cost-effective, stable, resistant to harsh environments, and more amenable to engineering at the molecular level than antibodies.[17] Denmeade et al. identified a specific peptide with the amino acid sequence HSSKLQ that can be used as a substrate to measure PSA enzymatic activity in extracellular fluids with a high degree of specificity and good stability.[18] Several peptide-based methods have been developed for the detection of PSA, such as

Received: September 19, 2013
Accepted: January 17, 2014
Published: January 17, 2014

   dx.doi.org/10.1021/ac402991r | *Anal. Chem.* 2014, 86, 1372−1379

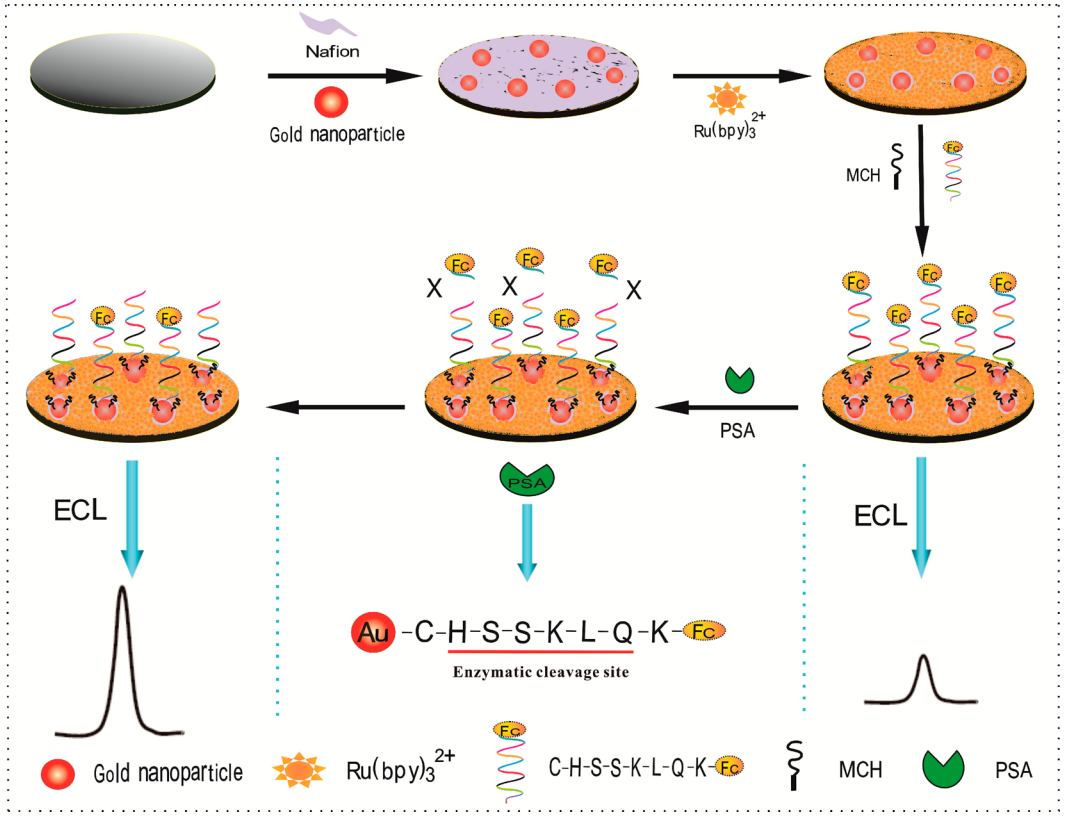

Figure 1. Schematic diagram of the fabrication process of ECL-PB biosensor for the determination of PSA.

fluorescence peptide-based assays,[19,20] electrochemical peptide-based assays,[21,22] and the ECL peptide-based assay.[23] The ECL method has attracted considerable attention for protein detection due to its high sensitivity, rapidity, easy controllability, and wide dynamic range.[24,25] Recently, we developed an ECL method for the determination of PSA by employing a specific peptide as molecular recognition element.[23] In our previous work,[23] the ECL biosensor was fabricated by self-assembling a specific peptide (CHSSKLQK) tagged with bis(2,2′-bipyridine)-4,4′-dicarboxybipyridine ruthenium-di(*N*-succinimidyl ester) bis(hexafluorophosphate) (Ru1-peptide) onto a gold electrode surface. PSA specifically cleaved the Ru1-peptide, resulting in the decrease of ECL signal. However, the sensitivity and linear range of the method developed in previous work were limited due to the high ECL background and inhibition model. Therefore, it is still necessary to develop more sensitive methods for the determination of PSA, especially in the point-of-care applications.

Here, we present an electrogenerated chemiluminescence peptide-based (ECL-PB) biosensor for the determination of PSA based on target-induced cleavage of specific peptide within Nafion films incorporated with gold nanoparticles (AuNPs) and ECL emitting species. The aim of this work is to augment the sensitivity of the ECL method for the determination of PSA. A specific peptide (CHSSKLQK, Figure S-1 in the Supporting Information) was designed according to ref 18 as a molecular recognition element that could be recognized and cleaved by PSA. Tris(2,2′-bipyridine) dichlororuthenium(II) ($Ru(bpy)_3^{2+}$) was used as an ECL emitting species because of its good chemical, electrochemical, and photochemical stability and higher luminescence yield.[26] Ferrocene carboxylic acid (Fc) was used as the ECL quencher to decrease the ECL intensity of the $Ru(bpy)_3^{2+}$-tri-*n*-propylamine (TPA) system.[27,28] Gold nanoparticles were used as the amplification platform because of their unique properties such as fascinating electrocatalytic activity, large surface area, excellent conductivity, and stability.[29] Figure 1 shows the schematic diagram of the fabrication process of ECL-PB biosensor for the determination of PSA. The ECL-PB biosensor was fabricated by casting the mixture of Nafion and AuNPs onto the surface of glassy carbon electrode to form AuNPs/Nafion film, and then, $Ru(bpy)_3^{2+}$ was electrostatically adsorbed into the AuNPs/Nafion film; finally, the peptide-tagged with ferrocene carboxylic acid (Fc-peptide) was self-assembled onto the surface of the AuNPs. When PSA was present, it specifically cleaved the Fc-peptide, leading the quencher to leave the electrode and resulting in the increase of the ECL intensity obtained from the resulted electrode in 0.1 M phosphate buffered saline (PBS, pH 7.4) containing TPA. In this work, the design and characteristics of the ECL-PB biosensor are discussed, and the analytical performance for the determination of PSA is presented.

EXPERIMENTAL SECTION

Fabrication of the ECL-PB Biosensor. Gold nanoparticles with a diameter of ~12 nm were prepared by citrate reduction of $HAuCl_4$ in aqueous solution according to ref 30. In brief, 100 mL of 0.01% $HAuCl_4$ was brought to reflux, and then, 4 mL of 1% sodium citrate was introduced while stirring. The gold nanoparticles suspension was then kept boiling for another 30 min and left to cool to room temperature.

A glassy carbon electrode (GCE, 2.0 mm diameter) was polished successively with 0.3, 0.05 μm alumina slurry (Beuhler), followed by rinsing thoroughly with water. The AuNPs−Nafion mixture was prepared by mixing 0.5% Nafion

dx.doi.org/10.1021/ac402991r | *Anal. Chem.* 2014, 86, 1372−1379

and the AuNPs suspension prepared above (v/v = 1:2) and sonicating for 30 min. Then, 10 μL of this mixture was spin-coated onto the surface of the cleaned GCE with a microsyringe and allowed to dry at room temperature to obtain AuNPs/Nafion modified GCE (AuNPs/Nafion/GCE). After that, AuNPs/Nafion/GCE was dipped into 1 mL of 1 mM $Ru(bpy)_3^{2+}$ for 30 min and then thoroughly rinsed with 10 mM phosphate buffer (PB, pH 7.4) to form an ECL layer of $Ru(bpy)_3^{2+}$/AuNPs/Nafion/GCE. A control $Ru(bpy)_3^{2+}$/Nafion modified GCE ($Ru(bpy)_3^{2+}$/Nafion/GCE) was fabricated as described above except without gold nanoparticles.

The ECL-PB biosensor was fabricated by dipping $Ru(bpy)_3^{2+}$/AuNPs/Nafion/GCE in 0.5 mL of 10 μM Fc-peptide solution for 40 min and then washed with 10 mM PB (pH 7.4) thoroughly. After that, the electrode was blocked with 1 mM 6-mercapto-1-hexanol (MCH) solution for 30 min. The resulting Fc-peptide/$Ru(bpy)_3^{2+}$/AuNPs/Nafion/GCE was then thoroughly washed with 10 mM PB (pH 7.4) and used as the ECL-PB biosensor.

ECL Measurement. The fabricated ECL-PB biosensor was immersed in 100 μL of 10 mM PB (pH 7.4) containing a fixed concentration of PSA or serum sample for 40 min, followed by a thorough washing with 10 mM PB (pH 7.4). A commercial cylindroid glass cell was used as an ECL cell, which contained a conventional three-electrode system consisting of a GCE, or a modified electrode or an ECL-PB biosensor as the working electrode, a platinum plate as the counter electrode, and an Ag/AgCl (saturated KCl) as the reference electrode, respectively. All potentials in this work were referred to the reference electrode. The ECL measurement was performed using a triangular potential scan with the rate of 100 mV/s in 1.0 mL of 0.1 M PBS (pH 7.4) containing 50 mM TPA. The concentration of PSA was quantified by an increased ECL intensity ($\Delta I = I_s - I_0$), where I_0 and I_S were the ECL intensity of the ECL-PB biosensor before and after incubation with PSA, respectively. All experiments were carried out at room temperature.

RESULTS AND DISCUSSION

Characterization of $Ru(bpy)_3^{2+}$ in AuNPs/Nafion Film. In this work, we employed gold nanoparticles as an ECL amplification platform to enhance the ECL signal of $Ru(bpy)_3^{2+}$. Prepared AuNPs were characterized by UV–vis adsorption spectrophotometry and transmission electron microscopy (TEM). The UV–vis adsorption spectrum of the prepared AuNPs (see Figure S-2A in the Supporting Information) shows the broad absorption at 520 nm, which is assigned to the characteristic resonance corresponding to the surface plasmon vibrations of the AuNPs.[31,32] The TEM image of the prepared AuNPs shows that gold nanoparticles maintain high levels of monodispersion and controlled size with an average diameter size of 12 nm (see Figure S-2B in the Supporting Information).

Figure 2A shows the ECL intensity–potential profiles at different electrodes in 0.1 M PBS (pH 7.4) containing 50 mM TPA. A low ECL signal at AuNPs/Nafion/GCE (c) is observed, which may be attributed to the oxidation of TPA in the presence of AuNPs.[33,34]The ECL intensity at the $Ru(bpy)_3^{2+}$/AuNPs/Nafion/GCE is 2.7-fold greater than that obtained at a $Ru(bpy)_3^{2+}$/Nafion/GCE. This indicates that AuNPs can enhance the ECL signal.

In order to understand the AuNPs amplification on the ECL signal, a series of the experiments was carried out including

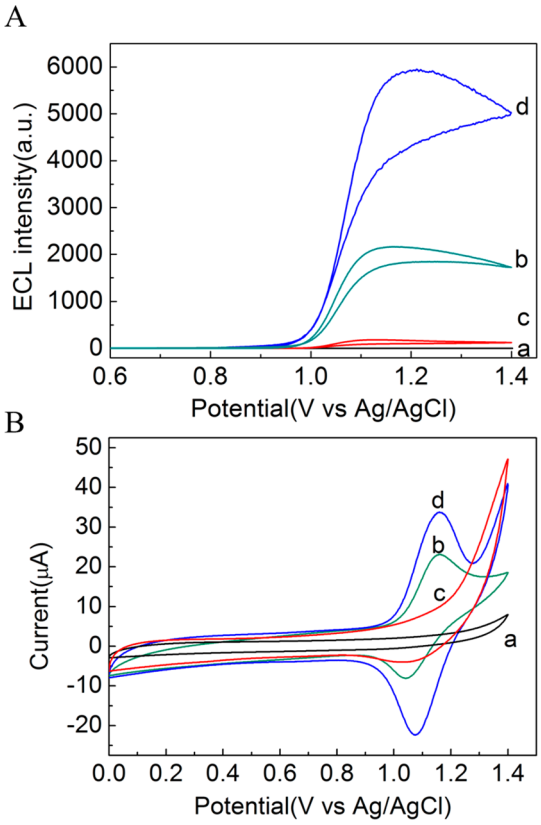

Figure 2. (A) ECL intensity–potential profiles obtained at different electrodes in 0.1 M PBS (pH 7.4) containing 50 mM TPA. (B) Cyclic voltammograms obtained at different electrodes in 0.1 M PBS (pH 7.4). (a) Nafion/GCE; (b) $Ru(bpy)_3^{2+}$/Nafion/GCE; (c) AuNPs/Nafion/GCE; (d) $Ru(bpy)_3^{2+}$/AuNPs/Nafion/GCE. Scan rate, 100 mV/s.

surface coverage of $Ru(bpy)_3^{2+}$, apparent diffusion coefficient of $Ru(bpy)_3^{2+}$, and ECL spectrum of bound $Ru(bpy)_3^{2+}$. Figure 2B shows the cyclic voltammograms obtained at different electrodes in 0.1 M PBS (pH 7.4). The cyclic voltammogram obtained at $Ru(bpy)_3^{2+}$/Nafion/GCE (b) is similar in shape to that at $Ru(bpy)_3^{2+}$/AuNPs/Nafion/GCE (d), showing well-defined redox waves at about +1.1 V, which is the characteristic redox wave of $Ru(bpy)_3^{2+}$.[35–37] The charging current appearing in the potential range of 0–1.0 V at AuNPs/Nafion/GCE (c) is larger than that at Nafion/GCE (a), and the oxidation peak current (d) obtained at the $Ru(bpy)_3^{2+}$/AuNPs/Nafion/GCE is 1.7-fold greater than that (c) obtained at the $Ru(bpy)_3^{2+}$/Nafion/GCE. The surface coverage of $Ru(bpy)_3^{2+}$ was estimated to be 1.2×10^{-8} mol/cm^2 at $Ru(bpy)_3^{2+}$/AuNPs/Nafion/GCE and 6.5×10^{-9} mol/cm^2 at $Ru(bpy)_3^{2+}$/Nafion/GCE, respectively, on the basis of the integrated oxidation charge values (with the correction of background). Similar results were reported at TiO_2–Nafion film,[35] CNTs–Nafion film,[36] and SiO_2–Nafion film.[37] This indicates that the interfusion of AuNPs can increase the load amount of $Ru(bpy)_3^{2+}$ in the Nafion film.

The peak potential separation ΔE ($\Delta E = E_{p,a} - E_{p,c}$) is about 70 mV at $Ru(bpy)_3^{2+}$/AuNPs/Nafion/GCE with a scan rate of 0.5 V/s. This is much bigger than that expected for a surface-confined species ($\Delta E = 0$).[38] The larger peak separation is generally indicative of slow electron transfer between the electrode and the $Ru(bpy)_3^{2+}$ in the film and film resistance effects.[39,40] The peak current–scan rate experiment shows that

dx.doi.org/10.1021/ac402991r | Anal. Chem. 2014, 86, 1372–1379

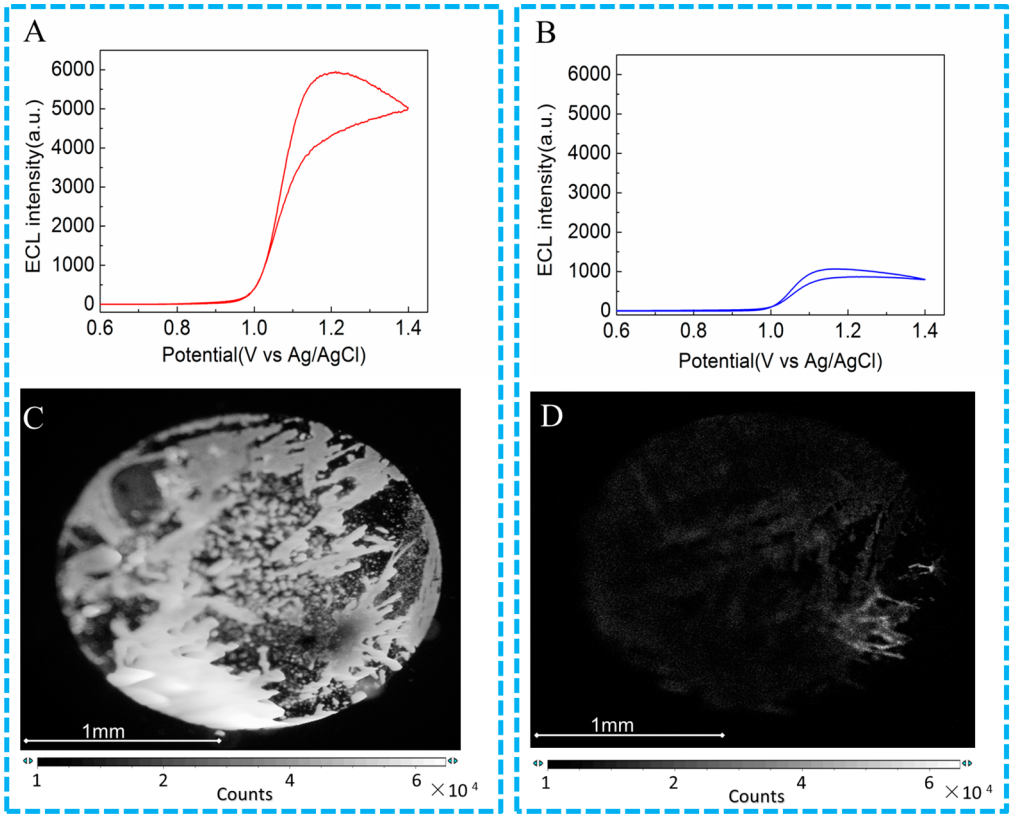

Figure 3. ECL intensity vs potential profiles (A, B) and ECL imaging (C, D) of $Ru(bpy)_3^{2+}$/AuNPs/Nafion/GCE (A, C) and the ECL-PB biosensor (B, D). Measurement solution, 0.1 M PBS containing 50 mM TPA (pH 7.4); scan rate, 100 mV/s. ECL imaging: exposure time, 16 s.

the peak current linearly increases with increasing scan rate at lower scan rates (<0.5 V/s), indicating that the electrode process of $Ru(bpy)_3^{2+}$ in the film has a surface behavior. It was also found that the peak current linearly increased with increasing the square root of the scan rate over the range from 0.5 to 5 V/s (see Figure S3 in the Supporting Information). This suggests that the electrode process of $Ru(bpy)_3^{2+}$ in the film is dominated by a diffusion step. On the basis of this, the apparent diffusion coefficient, D_{app}, for $Ru(bpy)_3^{2+}$ in the AuNPs/Nafion film was calculated to be 1.02×10^{-9} cm^2/s using the Randles−Sevcik equation.[35,40] This D_{app} is higher than that ($\sim 10^{-10}$ cm^2/s) reported for the $Ru(bpy)_3^{2+}$ in the pure Nafion film.[40] The uptake rate of $Ru(bpy)_3^{2+}$ into composite films is relatively fast (10 min) compared with that in pure Nafion film (25 min) under the identical experimental conditions. Therefore, the interfusion of AuNPs can lead to a faster diffusion of $Ru(bpy)_3^{2+}$ in the composite films.[35−37]

The normalized ECL spectra of $Ru(bpy)_3^{2+}$ at $Ru(bpy)_3^{2+}$/AuNPs/Nafion/GCE is similar to that in solution at GCE (see Figure S-4 in the Supporting Information). This may be attributed to the fact that Nafion could provide a polar environment which is similar to bulk solution.[41] This indicates that $Ru(bpy)_3^{2+}$ can maintain its ECL property in the tested films and process the coreactant ECL mechanism.[34,42] In summary, the interfusion of AuNPs can increase the load amount and lead to a faster diffusion of $Ru(bpy)_3^{2+}$ within the Nafion films.

In addition, it is worth-mentioning that the $Ru(bpy)_3^{2+}$/AuNPs/Nafion/GCE exhibits outstanding reproducibility under continuous scanning for 20 cycles by monitoring its ECL response in 0.1 M PBS (pH 7.4) containing 50 mM TPA with a relative standard derivation (RSD) of 2.3% (see Figure S-5 in the Supporting Information). The good reproducibility of the $Ru(bpy)_3^{2+}$/AuNPs/Nafion/GCE is attributed to the very large ion exchange selectivity coefficients (10^6−10^7) for hydrophobic ions such as $Ru(bpy)_3^{2+}$, thus preventing the immobilized reagent from leaching into solution.[43]

Characterization of Fc-Peptide in $Ru(bpy)_3^{2+}$/AuNPs/Nafion Film. The fabrication process of the ECL-PB biosensor was first characterized by cyclic voltammetry and electrochemical impedance spectrometry in the presence of the ferri/ferrocyanide redox couple as redox probe (see Figure S-6A,B in the Supporting Information). The oxidation peak current of ferricyanide decreased from 130.9 to 82.7 to 69.1 μA, and the peak potential separation ΔE increased from 83 to 104 to 180 mV for bare GCE, $Ru(bpy)_3^{2+}$/AuNPs/Nafion/GCE and Fc-peptide/$Ru(bpy)_3^{2+}$/AuNPs/Nafion/GCE, respectively (see Figure S-6A in the Supporting Information). This is mainly attributed to the fact that the peptide immobilized on the surface of the electrode prohibits the transfer of redox couple to the surface of electrode.

On the basis of the general electronic equivalent model of an electrochemical cell,[44] an equivalent circuit was proposed for the interpretation of the experimental impedance spectra of these modified electrodes (see Figure S-6 C in the Supporting Information). Q was added in this fit in order to improve the final fit and minimize errors. It can be seen that the simulating curves (dot) reproduce quite well the experimental data (line) (see Figure S-6 B in the Supporting Information). The R_{et} (271.8 Ω) extracted from the equivalent circuits at $Ru(bpy)_3^{2+}$/AuNPs/Nafion/GCE is bigger than that at bare GCE (20.8 Ω; see Table S-1 in the Supporting Information). The R_{et} at Fc-

dx.doi.org/10.1021/ac402991r | Anal. Chem. 2014, 86, 1372−1379

peptide/Ru(bpy)$_3^{2+}$/AuNPs/Nafion/GCE increased to 1068 Ω (Table S-1 in the Supporting Information). The EIS results also support that the Fc-peptide is modified on the Ru(bpy)$_3^{2+}$/AuNPs/Nafion/GCE. Comparing the square wave voltammogram obtained at the ECL-PB biosensor with that obtained at Ru(bpy)$_3^{2+}$/AuNPs/Nafion/GCE, a new peak current from the ECL-PB biosensor appears at +0.4 V (see Figure S-7 in the Supporting Information). This is attributed to the oxidation of Fc moiety in the Fc-peptide.

In order to study the way that the Fc-peptide is bound to the Ru(bpy)$_3^{2+}$/AuNPs/Nafion film, XPS is utilized for characterizing the surface compositions of Fc-peptide/AuNPs/Nafion film.[45] The XPS of Fc-peptide/AuNPs/Nafion film exhibits a pair of peaks at 83.9 and 87.6 eV (see Figure S-8 A in the Supporting Information), assigned to the Au 4f7/2 and Au 4f5/2 peaks,[46] respectively, indicating the existence of AuNPs. The XPS S 2p signal of Fc-peptide/AuNPs/Nafion film was fitted by two main components corresponding to the Au−S bond (162 eV) and unbounded sulfur (165 eV, Figure S-8B in the Supporting Information). The presence and shape of S 2p (162 eV) and Au 4f peaks confirm that Fc-peptide is self-assembled onto the AuNPs into the Nafion film by the Au−S bond. Additionally, the XPS data show that a fraction of Fc-peptide is physically adsorbed or trapped into Nafion film (S 2p 165 eV component).[47,48]

Figure 3 shows ECL intensity vs potential profiles at Ru(bpy)$_3^{2+}$/AuNPs/Nafion/GCE (A) and the ECL-PB biosensor (B). It is clearly seen that the ECL intensity decreases from 5911 (A) to 1050 (B) after Fc-peptide is self-assembled onto Ru(bpy)$_3^{2+}$/AuNPs/Nafion/GCE. We also observed the ECL quenching in solution and the fluorescence quenching of Ru(bpy)$_3^{2+}$ by Fc on Nafion film (see Figure S-9 in the Supporting Information), which is similar with that in refs 49 and 50. This is attributed to the ECL quenching of Fc in Fc-peptide, that is, bimolecular energy or electron transfer between Ru(bpy)$_3^{2+*}$ and ferrocenium (Fc^+), the oxidized species of Fc, along with suppression of radical reactions.[49] The effective ECL quenching of Ru(bpy)$_3^{2+}$ by the Fc can also be visually verified via ECL imaging, by comparing Figure 3C with Figure 3D. It should be noted that, in Figure 3C,D, the ECL signal is completely nonuniform on the surface of the electrode, attributed to the fact that the distribution of Ru(bpy)$_3^{2+}$ is not homogeneous in the AuNPs/Nafion film.[40] The effective quenching of Ru(bpy)$_3^{2+}$ by Fc-peptide provides a low background for the sensitive determination of PSA.

Figure 4 shows ECL intensity vs potential profiles and ECL imaging of the ECL-PB biosensor before and after the biosensor incubated with different concentrations of PSA, respectively. The ECL peak intensity greatly increases as the PSA concentration is elevated. This indicates that Fc-peptide is recognized and cleaved by target PSA,[18−23] resulting in the decrease of the amount of Fc on the electrode surface and, thus, a remarkable increase of ECL signal. The cleavage of Fc-peptide by PSA can also be visually verified via ECL imaging, as showed in Figure 4B−D. Therefore, the ECL-PB biosensor can be used to quantify PSA.

The dependence of the ECL intensity of the ECL-PB biosensor on the self-assembly time and cleavage time of Fc-peptide was investigated. As shown in Figure 5A, the ECL intensity sharply decreases with the increase of self-assembly time from 5 to 40 min. When the self-assembly time is prolonged from 40 to 60 min, the ECL intensity is nearly kept stable, attributed to the saturation of Fc-peptide. The

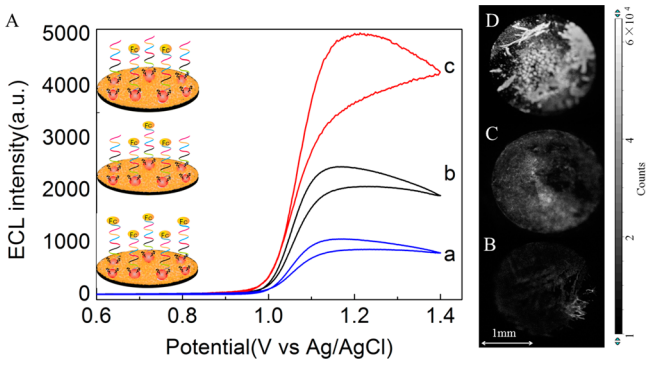

Figure 4. (A) ECL intensity vs potential profiles of the ECL-PB biosensor before (a) and after incubation with 5.0 × 10^{-11} g/mL PSA (b) and 5.0 × 10^{-9} g/mL PSA (c). ECL imaging of the ECL-PB biosensor before (B) and after incubation with 5.0 × 10^{-11} g/mL PSA (C) and 5.0 × 10^{-9} g/mL PSA (D). Measurement conditions are the same as those in Figure 3.

quenching ratio of Fc-peptide was calculated to be from 33% (at 5 min) to 82% (at 40 min), as shown in Figure 5B. Considering that a low background is beneficial for a low detection limit for the determination of PSA, we chose 40 min as the self-assembly time for 10 μM Fc-peptide in the following experiments.

Figure 5C displays the dependence of the ECL intensity on the cleavage time. The ECL intensity increased with increasing cleavage time from 5 to 30 min and reached a maximum at about 40 min. This indicates that the specific proteolytic cleavage event of Fc-peptide on the electrode surface in the presence of 5.0 × 10^{-11}g/mL PSA is completed within 40 min at room temperature. To obtain the high sensitivity, 40 min was set as the cleavage time in the following experiments.

Analytical Performance of the ECL-PB Biosensor. Figure 6 shows the ECL responses to different concentrations of PSA (A) and calibration curve of PSA (B). From Figure 6A, it is clearly seen that the ECL intensity gradually increases when the concentration of PSA is elevated from 5 pg/mL to 5 ng/mL with a good reproducibility in three times. The increased ECL intensity ΔI is directly proportional to the logarithm of the PSA concentration in the range from 5.0 × 10^{-12} to 5.0 × 10^{-9} g/mL (Figure 6B). The linear regression equation is ΔI = 1117 lgC + 13 277 (unit of C is g/mL) with the correlation coefficient of 0.9959. The detection limit is calculated to be 8 × 10^{-13}g/mL PSA (3σ).[51] This is 250-fold lower than that obtained by the electrochemical method using Fc-labeled peptide (2 × 10^{-10} g/mL)[21] and 47-fold lower than that obtained by the homogeneous ECL method using Ru1-peptide (3.8 × 10^{-11} g/mL)[23] (list of more methods in the Supporting Information, Table S-2). This detection limit is well below normal levels found in blood.[5,6] Such ultrasensitive detection may be useful for diagnosing prostate cancer in the postsurgery recurrence and also for the detection of breast cancer in women.[52]

The relative standard deviation (RSD) for 5.0 × 10^{-10} g/mL PSA was 4.3% (n = 5). The satisfied reproducibility is, therefore, evident. In this work, surprisingly, it is found that the ECL-PB biosensor exhibited outstanding reproducibility under continuous scan for 10 cycles with a RSD of 1.8% (see Figure S-10 in the Supporting Information). The response of the ECL-PB biosensors for 0.5 ng/mL PSA did not significantly change (less than 7%) when the biosensors were stored in air over 7

dx.doi.org/10.1021/ac402991r | Anal. Chem. 2014, 86, 1372−1379

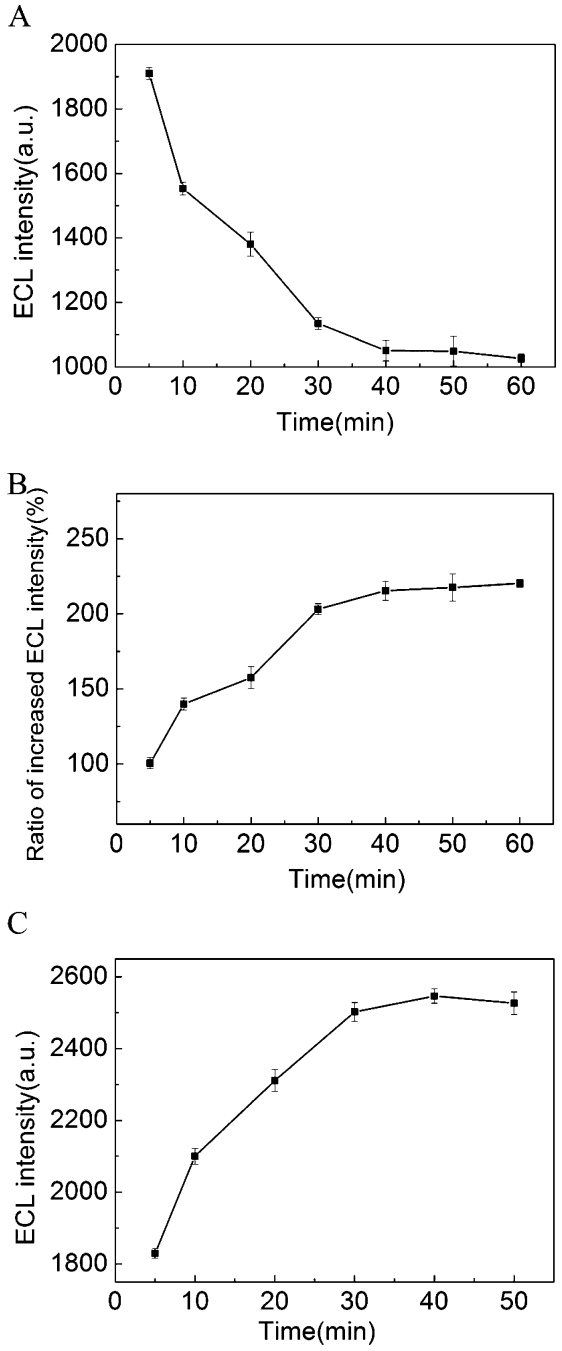

Figure 5. (A) Dependence of the blank ECL intensity of ECL-PB biosensor on the self-assembly time of 10 μM Fc-peptide, (B) dependence of the ratio of increased ECL intensity on the self-assembly time of 10 μM Fc-peptide, and (C) dependence of the ECL intensity of ECL-PB biosensor on cleavage time for 5.0×10^{-11} g/mL PSA. Measurement conditions are the same as those in Figure 3.

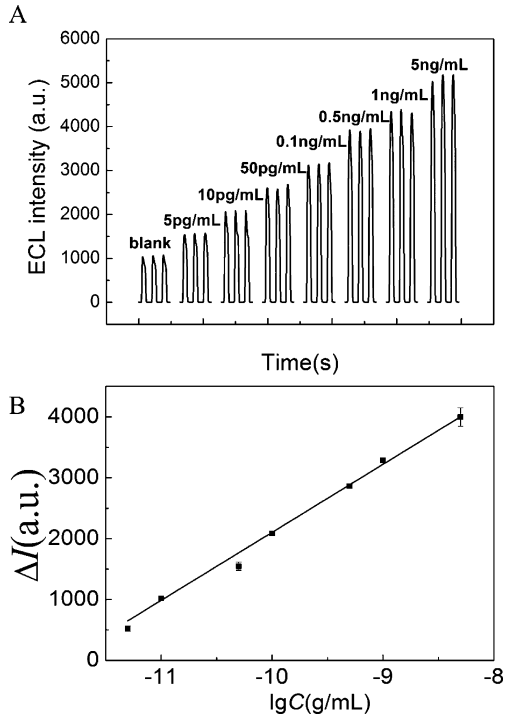

Figure 6. (A) ECL responses to different concentrations of PSA. (B) Calibration curve of PSA. Measurement conditions are the same as those in Figure 3.

days. This indicates that the proposed approach in our work is much better than only the thiol-Au self-assembled layer without Nafion film. The latter is attributed to the fact that the thiol compounds are easily desorbed from the electrode surface by electrochemical oxidation at the potentials of 0.9 V or higher and gradually degraded in air or in a PBS solution.[53] The good reproducibility and storage stability of the ECL-PB biosensor may be attributed to following reasons, such as, a high load amount of $Ru(bpy)_3^{2+}$ and Fc-peptide in AuNPs/Nafion/GCE, the storage stability of Fc-peptide in Nafion, and the very large ion exchange selectivity coefficients of Nafion preventing the immobilized reagents from leaching into solution.[43]

In order to demonstrate the gold nanoparticle amplification and the efficient immobilization of the cysteine-containing peptide in AuNPs/Nafion/GCE, three ECL-PB biosensors were fabricated. For the biosensor fabricated by direct physical adsorption of the Fc-peptide (CHSSKLQK-Fc) onto $Ru(bpy)_3^{2+}$/Nafion/GCE, the increased ECL intensity was directly proportional to the logarithm of the PSA concentration in the range from 5.0×10^{-10} to 5.0×10^{-8} g/mL (see Figure S-11 A in the Supporting Information). The regression equation was $\Delta I = 449$ lgC + 4484 (unit of C is g/mL) with a correlation coefficient of 0.9944. The detection limit was calculated to be 0.2 ng/mL. For the biosensor fabricated by adsorbing Fc-peptide1 (HSSKLQK-Fc) without cysteine at the end of peptide onto $Ru(bpy)_3^{2+}$/AuNPs/Nafion/GCE, the increased ECL intensity was directly proportional to the logarithm of the PSA concentration in the range from 1.0×10^{-10} to 1.0×10^{-8} g/mL (see Figure S-11 B in the Supporting Information). The regression equation was $\Delta I = 549$ lgC + 6018 (unit of C is g/mL) with a correlation coefficient of 0.960. The detection limit was 40 pg/mL. Additionally, the blank ECL intensity of Fc-peptide1/$Ru(bpy)_3^{2+}$/AuNPs/Nafion/GCE is much higher (3017) than that of Fc-peptide/$Ru(bpy)_3^{2+}$/AuNPs/Nafion/GCE (1050). The sensitivity (a slope of linear relationship between the increased ECL intensity and the logarithm of the PSA concentration, 1117) of the biosensor fabricated by self-assembly of Fc-peptide onto $Ru(bpy)_3^{2+}$/AuNPs/Nafion/GCE was higher than that by directly adsorbing Fc-peptide onto a $Ru(bpy)_3^{2+}$/Nafion/GCE (449) and by adsorbing Fc-peptide1 onto $Ru(bpy)_3^{2+}$/AuNPs/Nafion/GCE (549). The detection limit (8×10^{-13}g/mL) is much lower than that by directly adsorbing Fc-peptide onto a $Ru(bpy)_3^{2+}$/Nafion/GCE (0.2 ng/mL) and by adsorbing Fc-

dx.doi.org/10.1021/ac402991r | Anal. Chem. 2014, 86, 1372−1379

peptide1 onto $Ru(bpy)_3^{2+}$/AuNPs/Nafion/GCE (40 pg/mL). The employment of gold nanoparticles as amplification platform, the ECL background suppression through Fc as an ECL quencher to improve the sensitivity, and the efficient immobilization of the cysteine-containing peptide onto AuNPs/Nafion/GCE, therefore, are evident.

An evaluation of the selectivity of the ECL method was performed by examining 5.0×10^{-10} g/mL PSA or 5.0×10^{-9} g/mL other proteins, including four cancer biomarkers, C-reactive protein (CRP), Troponin I (TnI), human alpha-fetoprotein (AFP), and carcinoembryonic antigen (CEA), and two serum proteases such as trypsin and thrombin, respectively. Compared with the ECL intensity obtained in 0.1 M PBS containing 50 mM TPA (pH = 7.4), a great increase in the ECL intensity was observed for 5.0×10^{-10} g/mL PSA ($\Delta I/I_0$ = 170%), while very slight changes in the ECL intensity were found for the other tested proteins including CRP (4.0%), TnI (3.8%), AFP (2.7%), CEA (−5.6%), trypsin (4.6%), and thrombin (3.6%), respectively (see Figure S-12 in the Supporting Information). The results indicate that the ECL method developed in this work has a good selectivity.

The proposed method was also implemented in the analysis of clinical serum samples including four positive sera and four negative sera, which were provided by Xi'an Friendship Medical Inspection (China) according to the rules of the local ethical committee. The assay results are listed in Table 1. The obtained results showed an acceptable agreement with the data provided by Xi'an Friendship Medical Inspection (China) using a standard chemiluminescence (CL) method with an ECLIA-II Chemiluminescence Immunoanalyzer (Xiamen tianzhongda Polytron Technologies Inc., China), therefore, indicating a possibility in clinical application.

Table 1. Analytical Results of PSA in Clinical Serum Samples

sample number	CL method (ng/mL)[a]	this method (n = 3, P = 0.9, ng/mL)[b]	relative error (%)
1	1.08	1.06 ± 0.10	−1.5
2	1.12	1.17 ± 0.20	4.7
3	2.09	2.10 ± 0.36	0.3
4	3.53	3.55 ± 0.80	0.6
5	8.36	7.55 ± 1.23	−9.6
6	11.73	11.71 ± 1.53	−0.2
7	14.83	14.07 ± 1.77	−5.1
8	61.92	61.56 ± 6.78	−0.5

[a]The CL results of PSA in patients' serum samples from clinical reports provided by Xi'an Friendship Medical Inspection. [b]Confidence interval.

CONCLUSION

In this work, we developed an ultrasensitive ECL-PB biosensor for the determination of PSA on the basis of target-induced cleavage of a peptide. The ECL method measures PSA over a dynamic concentration range (5 pg/mL−5 ng/mL) with an extremely low detection limit of 0.8 pg/mL. Detection of PSA in serum sample indicates that the proposed ECL method is promising in clinical application. This approach provides the framework for the development of enzymatic cleavage-based ECL biosensors by employing the direct transduction of peptide cleavage events and an ECL method with high sensitivity and selectivity. It can be extended for the determination of other targets that display enzymatic cleavage activity, and the combination of the proposed approach with an ECL commercial bioanalyzer will be applied in point-of-care testing of other proteases.

ASSOCIATED CONTENT

Supporting Information

Materials, apparatus, twelve figures, and two tables as noted in the text. This material is available free of charge via the Internet at http://pubs.acs.org.

AUTHOR INFORMATION

Corresponding Authors

*E-mail: honglanqi@snnu.edu.cn. Phone: +86-29-81530726. Fax: +86-29-81530727.

*E-mail: cxzhang@snnu.edu.cn. Phone: +86-29-81530726. Fax: +86-29-81530727.

Notes

The authors declare no competing financial interest.

ACKNOWLEDGMENTS

We thank The National Science Foundation of China (Nos. 21375084, 21328501, 21275095, 21027007), the Natural Science Basic Research Plan in Shaanxi Province of China (No. 2013KJXX-73), Program for Changjiang Scholars and Innovative Research Team in University (IRT1070), The 111 project (No. B14041), and the Fundamental Research Funds for the Central Universities (No. GK201302050) for support. We also thank Haifeng Liu in Xi'an Friendship Medical Inspection for providing the CL results of the samples.

REFERENCES

(1) Lin, J.; Ju, H. *Biosens. Bioelectron.* **2005**, *20*, 1461−1470.
(2) Nadler, R. B.; Humphrey, P. A.; Smith, D. S. *J. Urol.* **1995**, *154*, 407−413.
(3) Diamandis, E. P. *Clin. Chem.* **2000**, *46*, 896−900.
(4) Kingsmore, S. F. *Nat. Rev. Drug Discovery* **2006**, *5*, 310−321.
(5) Stenman, U. H.; Leinonen, J.; Zhang, W. M.; Finne, P. *Semin. Cancer Biol.* **1999**, *9*, 83−93.
(6) Healy, D. A.; Hayes, C. J.; Leonard, P.; McKenna, L.; O'Kennedy, R. *Trends Biotechnol.* **2007**, *25*, 125−131.
(7) Yu, H.; Giai, M.; Diamandis, E. P.; Katsaros, D.; Sutherland, D. J. A.; Levesque, M. A.; Roagna, R.; Ponzone, R.; Sismondi, P. *Cancer Res.* **1995**, *55*, 2104−2110.
(8) Liu, D.; Huang, X.; Wang, Z.; Jin, A.; Sun, X.; Zhu, L.; Wang, F.; Ma, Y.; Niu, G.; Hight Walker, A. R.; Chen, X. *ACS Nano* **2013**, *7*, 5568−5576.
(9) Uludag, Y.; Tothill, I. E. *Anal. Chem.* **2012**, *84*, 5898−5904.
(10) Triroj, N.; Jaroenapibal, P.; Shi, H.; Yeh, J. I.; Beresford, R. *Biosens. Bioelectron.* **2011**, *26*, 2927−2933.
(11) Xu, S.; Liu, Y.; Wang, T.; Li, J. *Anal. Chem.* **2011**, *83*, 3817−3823.
(12) Zhang, Y.; Dai, W.; Liu, F.; Li, L.; Li, M.; Ge, S.; Yan, M.; Yu, J. *Anal. Bioanal. Chem.* **2013**, *405*, 4921−4929.
(13) Zhang, M.; Dai, W.; Yan, M.; Ge, S.; Yu, J.; Song, X.; Xu, W. *Analyst* **2012**, *137*, 2112−2118.
(14) Tian, C. Y.; Zhao, W. W.; Wang, J.; Xu, J. J.; Chen, H. Y. *Analyst* **2012**, *137*, 3070−3075.
(15) Sardesai, N. P.; Kadimisetty, K.; Faria, R.; Rusling, J. F. *Anal. Bioanal. Chem.* **2013**, *405*, 3831−3838.
(16) Niemela, P.; Lovgren, J.; Karp, M.; Lilja, H.; Pettersson, K. *Clin. Chem.* **2002**, *48*, 1257−1264.
(17) Petrenko, V. A.; Vodyanoy, V. J. *J. Microbiol. Methods* **2003**, *53*, 253−262.
(18) Denmeade, S. R.; Lou, W.; Lövgren, J.; Malm, J.; Lilja, H.; Isaacs, J. T. *Cancer Res.* **1997**, *57*, 4924−4930.

(19) Lee, K.; Mandal, S.; Morry, J.; Srivannavit, O.; Gulari, E.; Kim, J. *Chem. Commun.* **2013**, *49*, 4528−4530.
(20) Choi, J. H.; Kim, H. S.; Choi, J. W.; Hong, J. W.; Kim, Y. K.; Oh, B. K. *Biosens. Bioelectron.* **2013**, *49*, 415−419.
(21) Zhao, N.; He, Y.; Mao, X.; Sun, Y.; Zhang, X.; Li, C. Z.; Lin, Y. *Electrochem. Commun.* **2010**, *12*, 471−474.
(22) Roberts, M. A.; Kelley, S. O. *J. Am. Chem. Soc.* **2007**, *129*, 11356−11357.
(23) Qi, H.; Wang, C.; Qiu, X.; Gao, Q.; Zhang, C. *Talanta* **2012**, *100*, 162−167.
(24) Hu, L.; Xu, G. *Chem. Soc. Rev.* **2010**, *39*, 3275−3304.
(25) Miao, W. *Chem. Rev.* **2008**, *108*, 2506−2553.
(26) Tokel, N. E.; Bard, A. J. *J. Am. Chem. Soc.* **1972**, *94*, 2862−2863.
(27) Wang, X.; Dong, P.; Yun, W.; Xu, Y.; He, P.; Fang, Y. *Talanta* **2010**, *80*, 1643−1647.
(28) Li, Y.; Qi, H.; Peng, Y.; Gao, Q.; Zhang, C. *Electrochem. Commun.* **2008**, *10*, 1322−1325.
(29) Cao, X.; Ye, Y.; Liu, S. *Anal. Biochem.* **2011**, *417*, 1−16.
(30) Frens, G. *Nature* **1973**, *241*, 20−22.
(31) Duff, D. G.; Baikera, A.; Edwards, P. P. *J. Chem. Soc., Chem. Commun.* **1993**, 96−98.
(32) Patil, S.; Datar, S.; Rekha, N.; Asha, S. K.; Dharmadhikari, C. V. *Nanoscale* **2013**, *5*, 4404−4411.
(33) Kumar, S. S.; Bard, A. J. *Anal. Chem.* **2013**, *85*, 292−295.
(34) Zu, Y.; Bard, A. J. *Anal. Chem.* **2000**, *72*, 3223−3232.
(35) Choi, H. N.; Cho, S. H.; Lee, W. Y. *Anal. Chem.* **2003**, *75*, 4250−4256.
(36) Guo, Z.; Dong, S. *Anal. Chem.* **2004**, *76*, 2683−2688.
(37) Khramov, A. N.; Collinson, M. M. *Anal. Chem.* **2000**, *72*, 2943−2948.
(38) Laviron, E. *J. Electroanal. Chem.* **1979**, *101*, 19−28.
(39) Peerce, P. J.; Bard, A. J. *J. Electroanal. Chem.* **1980**, *114*, 89−115.
(40) Martin, C. R.; Rubinstein, I.; Bard, A. J. *J. Am. Chem. Soc.* **1982**, *104*, 4817−4824.
(41) Rubinstein, I.; Bard, A. J. *J. Am. Chem. Soc.* **1981**, *103*, 5007−5013.
(42) Chen, Z.; Zu, Y. *Langmuir* **2007**, *23*, 11387−11390.
(43) Szentirmay, M. N.; Martin, C. R. *Anal. Chem.* **1984**, *56*, 1898−1902.
(44) Barsoukov, E.; Macdonald, J. R. *Impedance Spectroscopy Theory, Experiment, and Applications*; Wiley: New York, 2005.
(45) Cho, T. J.; Zangmeister, R. A.; Maccuspie, R. I.; Patri, A. K.; Hackley, V. A. *Chem. Mater.* **2011**, *23*, 2665−2676.
(46) Moulder, J. F.; Stickle, W. F.; Sobol, P. E.; Bomben, K. D. *Handbook of X-ray Photoelectron Spectroscopy*; Perkin-Elmer: Eden Prairie, MN; 1992.
(47) Weisbecker, C. S.; Merritt, M. V.; Whitesides, G. M. *Langmuir* **1996**, *12*, 3763−3772.
(48) Menéndez, G. O.; Cortés, E.; Grumelli, D.; Méndez De Leo, L. P.; Williams, F. J.; Tognalli, N. G.; Fainstein, A.; Vela, M. E.; Jares-Erijman, E. A.; Salvarezza, R. C. *Nanoscale* **2012**, *4*, 531−540.
(49) Cao, W.; Ferrance, J. P.; Demas, J.; Landers, J. P. *J. Am. Chem. Soc.* **2006**, *128*, 7572−7578.
(50) Lee, E. L.; Wrighton, M. S. *J. Am. Chem. Soc.* **1991**, *113*, 8562−8564.
(51) Kaiser, H. *Pure Appl. Chem.* **1973**, *34*, 35−62.
(52) Grubisha, D. S.; Lipert, R. J.; Park, H. Y.; Driskell, J.; Porter, M. D. *Anal. Chem.* **2003**, *75*, 5936−5943.
(53) Sun, B.; Qi, H.; Ma, F.; Gao, Q.; Zhang, C.; Miao, W. *Anal. Chem.* **2010**, *82*, 5046−5052.